Geophysical Research Letters

RESEARCH LETTER
10.1029/2019GL085452

The Köppen-Trewartha Climate-Type Changes Over the CORDEX-East Asia Phase 2 Domain Under 2 and 3 °C Global Warming

Sera Jo[1], Joong-Bae Ahn[1,2], Dong-hyun Cha[3], Seung-Ki Min[4], Myoung-Seok Suh[5], Young-Hwa Byun[6], and Jin-Uk Kim[6]

[1]Department of Atmospheric Sciences, Pusan National University, Busan, South Korea, [2]Now at Climate Prediction Laboratory, Department of Atmospheric Sciences, Pusan National University, Busan, South Korea, [3]Ulsan National Institute of Science and Technology, Ulsan, South Korea, [4]Division of Environmental Science and Engineering, Pohang University of Science and Technology, Pohang, South Korea, [5]Department of Atmospheric Sciences, Kongju National University, Kongju, South Korea, [6]Climate Research Division, National Institute of Meteorological Research, Jeju, South Korea

Key Points:
- Baseline assessment of climate change over East Asia under the 2 and 3 °C global warming is here presented
- Of the East Asia region, 17.6% (25.2%) is expected to experience major climate-type changes under the 2 and 3 °C global warming
- The changes are accompanied by intensified hydroclimatic stress and have statistically significant trends until the end of the 21st century

Supporting Information:
- Supporting Information S1

Correspondence to:
J.-B. Ahn,
jbahn@pusan.ac.kr

Citation:
Jo, S., Ahn, J.-B., Cha, D.-h., Min, S.-K., Suh, M.-S., Byun, Y.-H., & Kim, J.-U. (2019). The Köppen-Trewartha climate-type changes over the CORDEX-East Asia phase 2 domain under 2 and 3 °C global warming. *Geophysical Research Letters*, *46*, 14,030–14,041. https://doi.org/10.1029/2019GL085452

Received 18 SEP 2019
Accepted 23 NOV 2019
Accepted article online 3 DEC 2019
Published online 6 DEC 2019

Abstract For the comprehensive estimation of regional climate change over East Asia (EA) at the 2 and 3 °C global warming levels (GWLs), the Köppen-Trewartha climate-type change is assessed with ensemble regional climate change projections in line with Coordinated Regional Climate Downscaling Experiment (CORDEX)-EA phase 2. Under the 2 °C (3 °C) GWL, 17.6% (25.2%) of the EA region is expected to undergo major climate-type changes. Tropical and subtropical climate types will expand northward, accompanied by increasing hydroclimatic intensity. Limiting GWL to 2 °C shows benefits by preventing subtropical-type expansion around far EA. Desertification over inland regions of EA exhibits scenario dependency. Boreal and tundra climate types over high-latitude regions will tend to decrease rapidly, especially over the Tibetan Plateau. The results are expected to be a baseline assessment of climate change over EA under the 2 and 3 °C GWLs above the preindustrial level.

Plain Language Summary This paper investigates the Köppen-Trewartha climate-type changes over East Asia (EA) at the 2 and 3 °C global warming levels (GWLs) with the ensemble regional climate simulations. Under the 2 °C (3 °C) GWL, 17.6% (25.2%) of the EA region is expected to undergo major climate-type changes. The result shows increased tropical, subtropical, and desert climate types accompanied by intensification of hydroclimatic stress. In addition, boreal and tundra climate types over high-latitude regions will tend to decrease rapidly, especially over the Tibetan Plateau under the 2 and 3 °C GWLs.

1. Introduction

The United Nations Framework Convention on Climate Change Paris Agreement of December 2015 sets the mitigation goal of holding the global warming level (GWL) well below 2 °C compared to preindustrial (PI) levels and pursuing efforts to limit it to the 1.5 °C level (United Nations, 2015). However, considering carbon inertia and complex feedbacks, there exist skeptical views on the success of limiting GWL below 2 °C (e.g., Mauritsen & Pincus, 2017; Rogelj et al., 2016; Raftery et al., 2017; Knutti & Rogelj, 2015). In line with the 2015 Paris agreement, for instance, the signatories pronounced practical plans for reducing greenhouse gas (GHG) emissions, the so-called "intended nationally determined contributions" (INDCs), to prevent the irreversible anthropogenic climate change. Rogelj et al. (2016) examined the global GHG emissions based on INDCs and presented 2.6–3.1 °C warming by 2100. Raftery et al. (2017) also suggested a global temperature increase in 2100 within the range from 2.0 to 4.9 °C based on statistically estimated future emission levels. Therefore, a target temperature warmer than the goal of the 2015 Paris agreement should be examined for the realistic future.

Meanwhile, the regional climate does not respond monotonically to global warming (James et al., 2017; Kirtman et al., 2013; Seneviratne et al., 2016; Sillmann et al., 2013). Therefore, extensive research on the regional climate response to the target GWL has been conducted based on the general circulation model (GCM, sometimes global climate model) in various regions: King et al. (2017) and Lewis et al. (2017) for

Australia; King and Karoly (2017) and Vautard et al. (2014) for Europe; Osima et al. (2018) and Nkemelang et al. (2018) for Africa; Swain and Hayhoe (2015) and Karmalkar and Bradley (2017) for the United States; Xu et al. (2017), Chen and Sun (2018), Lee and Min (2018), Lee et al. (2018), Shi et al. (2018), and Zhao and Zhou (2019) for East Asia (EA).

However, GCMs have a weak point in resolution for reflecting the realistic impacts of local forcing with detailed topography or land use types (Ahn et al., 2016; Choi et al., 2016; Im et al., 2006, 2007, 2015; Lee & Hong, 2014). Therefore, numerous dynamically downscaled climate change assessments at the target GWL based on the regional climate model (RCM) have actively been carried out in line with the Coordinated Regional Climate Downscaling Experiment (CORDEX) project: Donnelly et al. (2017), Dosio and Fischer (2018), Jacob et al. (2018), and Marx et al. (2018) for the EURO-COREX domain; and Sylla et al., 2018, Sylla et al., 2018), Nikulin et al. (2018), Maúre et al. (2018), Mba et al. (2018), and Lennard et al. (2018) over the CORDEX-Africa domain.

The CORDEX-EA phase 2 (CORDEX-EA2) domain covers broader areas than do the general concept of EA, including the Asian-Pacific monsoon regions (e.g., Indian Monsoon, Western North Pacific Monsoon, and East Asian Monsoon; Wang & Lin, 2002), Mongolia, southern Russia, and eastern Kazakhstan (http://cordex-ea.climate.go.kr/cordex/area.do). This region is one of the most vulnerable regions under the target GWL due to its possible exposure to more frequent extreme heat events (Prajapat et al., 2019, for India; Shi et al., 2018, for China; Im et al., 2019, for South Korea [S. Korea]), increased heat stress (Lee & Min, 2018), and intensified precipitation (Ge et al., 2019, for Southeast Asia; Sun et al., 2018, for China). However, these studies have only partially examined these changes due to their focus on different regions and climatic variables. In order to understand the impact of the target GWL on the environment of EA, comprehensive analyses that consider the changes of climatic variables are needed. The Köppen climate classification is an efficient tool that offers the advantage of combining climatic variables (temperature and precipitation) and their seasonality within a single metric (Belda et al., 2015; Mahlstein et al., 2013). Since this metric has a threshold that considers plant sensitivity, it can be used as a baseline estimation of feasible biomes and ecosystem changes. In addition, it has broad applicability because the required data are common variables in climate models. Therefore, the Köppen scheme is used widely for climate change impact research with Special Report on Emission Scenarios (SRES; e.g., Gallardo et al., 2013; De Castro et al., 2007; Gao & Giorgi, 2008; Feng et al., 2012) and Representative Concentration Pathway (RCP) scenarios (e.g., Rajaud & de Noblet-Ducoudré, 2017; Chan & Wu, 2015; Zeroual et al., 2019; Mahlstein et al., 2013). A few studies have assessed Köppen-related climate-type changes over EA, merely focused on a relatively small area in the CORDEX-EA2 domain (i.e., Shi et al., 2012, and Chan et al., 2016, for China; Yun et al., 2012, and Lee et al., 2017, for S. Korea; Talchabhadel & Karki, 2019, for Nepal) using different emission scenarios, horizontal resolutions, and analysis periods. Since the differences in the projection domain (Bhaskaran et al., 2012; Leduc & Laprise, 2009; Žagar et al., 2013), horizontal resolution (Shi et al., 2018; Evans & McCabe, 2013), or model sensitivity to GHG forcing (Nikulin et al., 2018; Sylla, Pal, et al., 2018) could be the source of the uncertainty in regional climate projections, it is important to coordinate experiments and assess the future projection from the same baseline (e.g., PI level). Therefore, this study examines the Köppen-Trewartha (K-T) climate-type changes over the CORDEX-EA2 domain at 2 and 3 °C GWL from the PI level with the state-of-the-art GCM-RCM downscale chain forced by RCP4.5 and 8.5 scenarios.

2. Data and Method

2.1. Data

Under the framework of the national project of S. Korea, dynamical downscaling of Coupled Model Intercomparison Project (CMIP) Phase 5 GCM experiments is conducted by the collaboration of three different institutes in S. Korea in line with the CORDEX-EA2 project. For representing possible ranges of climate change, two different GCMs of CMIP5 are chosen for lateral boundary conditions: the Hadley Centre Global Environment Model version 2–Atmosphere-Ocean (HadGEM2-AO; Baek et al., 2013) operated by the National Institute of Meteorological Research/Korean Meteorological Administration and the Max Planck Institute Earth System Model Low Resolution (MPI-ESM-LR; Giorgetta et al., 2013). In terms of model genealogy (Knutti et al., 2013; Masson & Knutti, 2011), which quantitatively classified the CMIP3/5 GCMs into "family trees" by hierarchical clustering based on model characteristics (e.g., mean bias

pattern), The HadGEM2 and MPI-ESM models are distinguished as a different "family" among CMIP5 GCMs. Moreover, those two GCMs are assessed to have superior performance over the EA region compared to the other models (McSweeney et al., 2015). Thus, this combination of driving GCMs is expected to gratify the requirement for ensemble members to estimate climate changes in EA. The multimodel high-resolution regional climate projections that are analyzed in this study are HadGEM2-AO/RegCM, MPI-ESM-LR/WRF, and MPI-ESM-LR/CCLM with the same horizontal resolution (25 km) and domain configuration (Table S1 in the supporting information). As reference data of the present climate, Asian Precipitation–Highly Resolved Observational Data Integration Toward Evaluation of Water Resources (APHRODITE; Yatagai et al., 2012) daily gridded temperature and precipitation data are used with 0.25° × 0.25° horizontal resolution. The downscaled results have finer resolution than have APHRODITE; therefore, it is expected to be sufficient for describing the detailed climate-type distribution and resolve the complexity of climate in EA better than can the GCM results (Fig. S1).

2.2. Target GWL

The period reaching target GWLs is defined with global mean surface temperature (GMST) calculated from driving GCMs (HadGEM2-AO and MPI-ESM-LR). The PI level is usually defined as time-averaged GMST within the period of 1850–1900 (Collins et al., 2013; Hawkins et al., 2017; Joshi et al., 2011; Vautard et al., 2014). In this study, due to data availability, time-averaged GMST of historical experiments during 1861–1900 of each GCM is used as the PI baseline (Figure S2). The target warming period is defined as the timing that 25-year moving-average (central year) GMST reaches the target GWL. The 2 °C warming period is defined as 2030–2054 (2031–2055) for HadGEM2-AO and 2031–2055 (2024–2048) for MPI-ESM-LR under the RCP 4.5 (RCP8.5) scenario, respectively. As for the 3 °C GWL, only the RCP 8.5 scenario reaches the target level, and the period is 2050–2074 and 2049–2073 for HadGEM2-AO and MPI-ESM-LR, respectively. As for the 3 °C GWL, only the RCP 8.5 scenario reaches the target level, and the period is 2060–2084 and 2056–2080 for HadGEM2-AO and MPI-ESM-LR, respectively. In this study, therefore, the RCP8.5 scenario is primarily analyzed for the 2 and 3 °C target GWLs. RCP4.5 will be used in changing trend analysis (Figure 3), and other RCP4.5 results are added in the supporting information. Owing to the different sensitivity to GHG emission forcing between GCMs, the target warming period and the reference period are usually defined by each GCM, individually (Sylla, Faye, et al., 2018; Sylla, Pal, et al., 2018). However, in this study, a fixed reference period (1981–2005) is used because of data availability. According to the Intergovernmental Panel on Climate Change (IPCC) Special Report on Global Warming of 1.5 °C in 2018 (IPCC, 2018; hereafter IPCC SR 2018), GMST is increased by about 0.57–0.73 °C during 1986–2005 from the PI period (during 1850–1900), as estimated by various reanalysis data. As for HadGEM2-AO and MPI-ESM-LR, 0.48 and 0.84 °C increases of GMST, respectively, are projected, and the weighted GCM ensemble (Figure S2c) shows 0.72 °C warming from the PI period (1861–1900) during 1981–2005. By considering the different definitions of the PI (which contains a warmer period than IPCC SR 2018) and reference (which includes a cooler period than IPCC SR 2018) periods, the reference period of this study lies within the range of data sensitivity and remains reasonably representative of the current state of climate classification.

2.3. Method

The K-T scheme, which is a modified version of the original Köppen climate classification (Köppen, 1936), is utilized to estimate the climate change over EA (Table S2). The K-T method revises the original criteria and thereby achieves better agreement in the boundaries of natural landscapes than does the original Köppen classification (Belda et al., 2015; Trewartha & Horn, 1980).

As presented in Table S2, the K-T classification uses raw temperature and precipitation rather than anomaly when defining thresholds. Therefore, the results are crucially affected by the model biases, and so we applied a bias correction method, quantile delta mapping (QDM), based on cumulative distribution function matching. Quantile mapping is a powerful bias correction method for adjusting not only mean but also variance and extreme distributions (Chen et al., 2013; Eum & Cannon, 2017; Teutschbein & Seibert, 2012). However, it has disadvantages when applied to the future climate change data because of the stationary assumption that artificially offsets the model-projected trends (Hagemann et al., 2011; Maraun et al., 2017; Maurer & Pierce, 2014). To overcome this defect, QDM has been developed to conserve projected relative changes in quantiles (Bhatia et al., 2019; Cannon et al., 2015; Eum & Cannon, 2017). A detailed description of QDM is available in Appendix A of Cannon et al. (2015). Transfer functions for QDM are established

for each month based on daily precipitation and temperatures during historical, 2 °C warming, and 3 °C warming periods. In order to apply the QDM and ensemble analysis, model data are interpolated into the APHRODITE data grid system with rectilinear interpolation. The ensemble mean (ENS) is derived with the simple composite mean method with even weighting.

Precipitation changes are also analyzed with respect to climate indices derived from daily mean precipitation. Indices follow the definitions of the Expert Team on Climate Change Detection and Indices (ETCCDI; Karl et al., 1999; Peterson et al., 2001). We select the maximum length of dry spell (CDD), simple precipitation intensity index (SDII), and annual total precipitation above the 95th percentile threshold (R95pTOT) from ETCCDI to represent dry and wet precipitation extremes. Additionally, the hydroclimatic intensity index (HYINT; Giorgi et al., 2011, 2014; Im et al., 2017) is used to assess the changes of hydroclimatic stress in the target warming climate. Each climate index is defined in Table S4.

3. Results

3.1. Reference Period

EA has diverse climate types classified in terms of the K-T scheme in the reference period (Figure 1a). The southern regions of 20 °N are mainly covered by Aw types and the southern islands of the Philippines are included in the Ar climate zone. The western part of India exhibits steppe (Bs) climate, and the southern part of China is dominated by Cr- and Cw-type climates. Far EA (FEA), including the Korean Peninsula, Japan, and the northeastern part of China, is represented by D-type climate. Southern Mongolia and the northern part of China are described as desert climate (Bw). Regions northward of 50°N are principally covered with subarctic (E) climate, except for the eastern part of Kazakhstan. The Tibetan Plateau (TP), the so-called "Third Pole" of the Earth, is mostly classified into FT (tundra) climate and mixed with E (subarctic) and Bw (desert) climate types. Figure 1b denotes the K-T climate-type distribution of the ENS reference period after bias correction. Only few grid points present different climate types compared with APHRODITE (differences are not shown), indicating that the bias-corrected RCM can simulate EA climate types reasonably well compared with reanalysis data (Figure S3).

3.2. Future Climate at Target GWL

Under the 2 °C (3 °C) warmed climates forced by the business-as-usual scenario, 17.6% (25.2%) of the EA region is expected to undergo major climate-type changes (Figures 1c–1f and Table S3). One of the largest climate-type changes is from E to D climate type (Figure 2a), which is prevalent over high-latitude regions of EA around the southeastern part of Russia (Figures 1c–1f). The changes of precipitation indices such as CDD, SDII, R95pTOT, and HYINT are relatively small than those of other regions but show high consistency between ensemble members in terms of increased precipitation (Figures S5c and S5d), especially under the 3 °C GWL.

The FEA region covering the Korean Peninsula, central and southern Japan, and the middle of the North China Plain (NCP) is famous for highly populated regions with mega cities. This region exhibits changes from temperate (D) to subtropical (C) climate. The southern boundary of the temperate climate zone (D type) is projected to shrink northward due to the expansion of subtropical climate (C). These are supported by the previous studies, assessed under the SRES A1B scenario (Shi et al., 2012; Yun et al., 2012) and other RCP scenarios (Lee et al., 2017) at the end of the 21st century. These changes were accompanied by increases of both CDD (Figure 2b) and extreme precipitation intensity (Figures 2c and 2d), which increased the hydroclimatic stress (HYINT) (Figure 2e). The middle of the NCP shows this changing trend both under the 2 and 3 °C GWLs. If GMST is kept well below the 2 °C GWL, however, these climate-type distribution changes are expected to occur over only areas along the coastal line of the Korean Peninsula and the southern part of Japan (Figure 1d).

Over South Asia (SA), one of the most populous regions in the world, there are narrow bands of the subtropical climate zone along the Ganges River Valley and around the Madhya Pradesh state and the northern part of Indo-China Peninsula during the reference climate (Figures 1a and 1b). These regions have already started to experience the effect of climate change (e.g., a record-breaking heat wave over India that claimed about 5,000 casualties in 2018). Moreover, this region has high vulnerability for climate change because people's living primarily depends on outdoor work such as fishery or agriculture. Our result showed that these

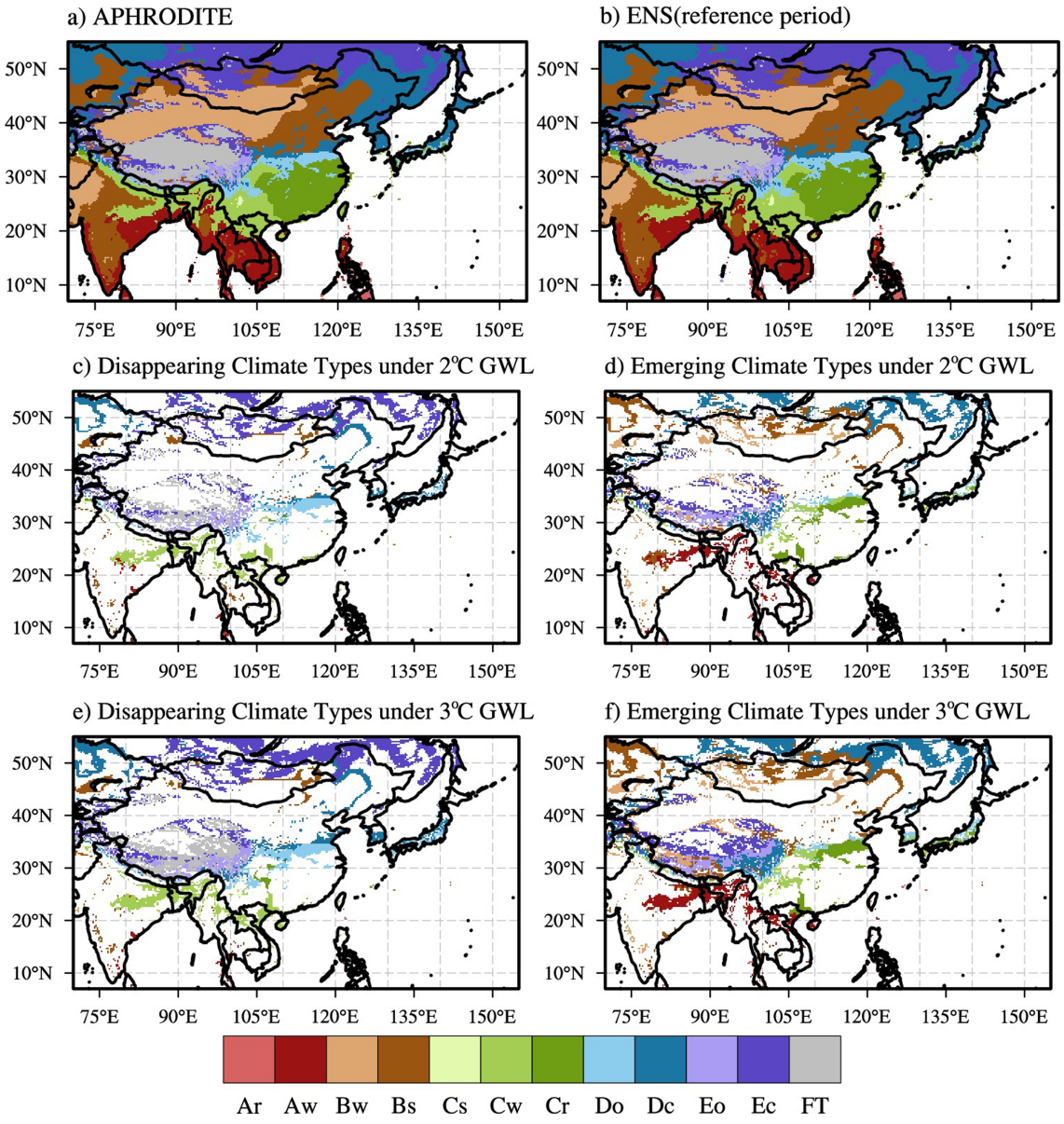

Figure 1. K-T climate-type map over CORDEX-EA2 domain derived from (a) APHRODITE and (b) ENS (reference period). Disappearing and emerging climate types of ENS in the (c, d) 2 °C and (e, f) 3 °C GWLs under the RCP8.5 scenario.

subtropical regions, including the Ganges River Valley and the Assam region of India, Myanmar, Laos, the Republic of Bangladesh, and the Hainan island of China, are projected to shift toward tropical humid climate (Figures 1c–1f). This major climate shift toward warmer and wetter climate than the current state indicates that the corresponding regions will be exposed to a more favorable condition in terms of high wet-bulb temperature, which is directly related to human survivability (Sherwood & Huber, 2010).

On the other hand, the dry area (B) at the midlatitude expands toward the northern part of Mongolia and some eastern parts of Kazakhstan and some B climate boundaries of India and the TP. The extended areas account for about 15% (30%) under the 2 °C (3 °C) GWL compared to the reference period (Figures 1c–1f and 3b). Given that these areas can be the source of yellow dust over EA countries, the expansion of these dry areas is likely to impact on the local environmental change, as well as have a remote impact on air quality at the lee-side countries in the future. Furthermore, following the eastern edge of steppe climate (Bs) in the reference period over northeast China, the dry climate tends to expand more eastward with a decrease of D climate types (Figures 1d and 1f). These regions including the three provinces of northeast China, that is,

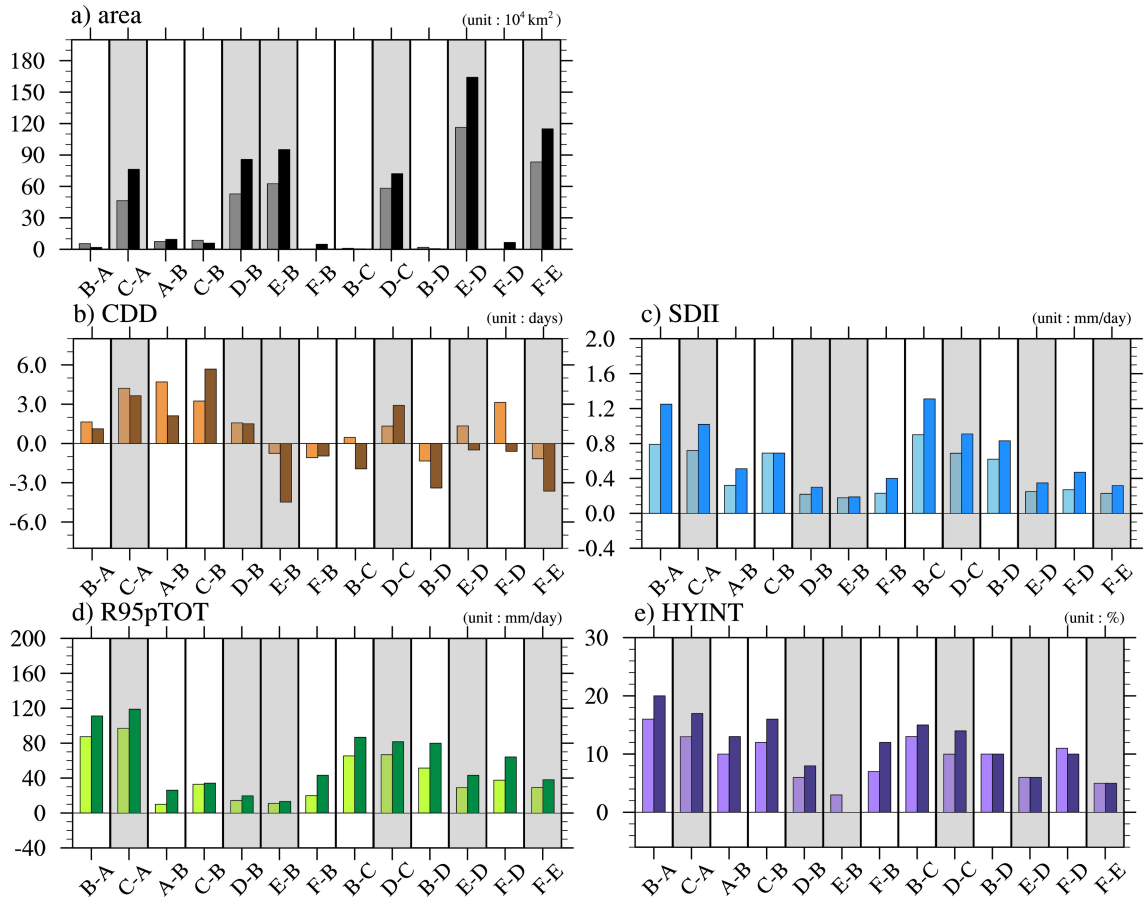

Figure 2. (a) Total area (unit: 10^4 km^2) and (b–e) extreme indices changes (compared to reference period) to the 2 °C (light colored bar) and 3 °C (dark colored bar) GWLs with respect to each major climate-type change. The shaded columns indicates that the changed area is larger than 1% of the whole CORDEX-EA2 (~2,532 × 10^4 km^2).

Heilongjian, Jilin, and Liaoning, which are the primary breadbaskets of corn production in the world, implying that the extension of B climate under the 2 °C GWL can be linked to food security and socioeconomic problems.

The most dramatic climate change over EA is projected over the TP. F climate type, which only exists over the TP region in EA, will experience K-T-type changes from FT to various types (B, D, and E), and the largest portion of FT-type loss is shifted toward E climate types (Fig. 2). These are in line with results with 18 CMIP5 GCMs (Chan et al., 2016). Areas of changing climate types from F show decreased CDD, except for F-D change in the 2 °C GWL (Figure 2b), and increased extreme precipitations (Figures 2c and 2d) and HYINT (Figure 2e), but with high uncertainty (the various ensemble members show disagreement on the sign of precipitation change) especially under the 3 °C GWL (Figures S5c and S5d).

3.3. Pace of Climate-Type Shift

So far, the analyses are based on a specific time slice within the long-term climate change. Nevertheless, the pace of shift is the critical information for the adaptation of species (Mahlstein et al., 2013; Sandel et al., 2011). Figure 3 displays the temporal evolution of area change (%) for each major climate type from the reference period to the end of the 21st century under each RCP scenario. The statistical significance of the slope is evaluated based on the Student *t* test. Tropical climate type (A) shows a persistent increase of about 1% per 5-year period in both RCP4.5 and RCP8.5 scenarios (Figure 3a). The area change of A climate type keeps increasing and becomes even sharper after the mid-21st century (2046–2070) under the RCP4.5 scenario, although RCP4.5 is a "stabilizing" scenario (van Vuuren et al., 2011). The main region of increased A climate type is SA (Figure 1), which has already experienced impact of climate change on the human

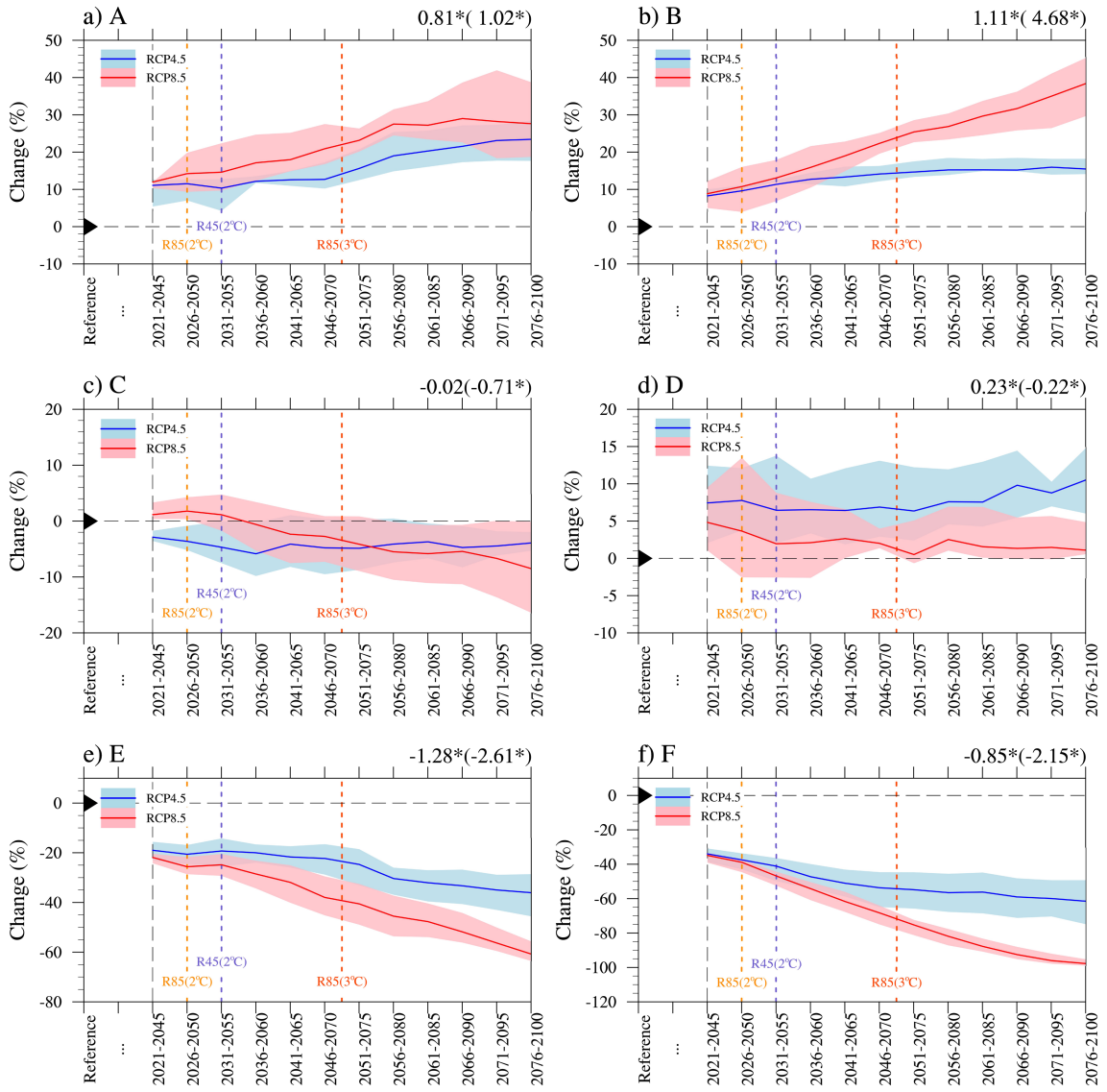

Figure 3. Time series of K-T type area changes with respect to the reference period (%: km^2/km^2) from 25-year-averaged climatology with moving central year in 5-year intervals. Thick line = ENS; shaded area = spread of ensemble members; dotted vertical lines with labels = target GWL reaching year (Fig. S2). The values in the upper right corner are the slope of ENS (%/5 years; * = 95% confidence level) under the RCP4.5 (RCP8.5) scenario.

survivability. The rapid rate of climate-type shift can result in severe climate crisis without time for adjustment in such regions. The most noticeable changing rate is found with B climate types (Figure 3b) under the RCP8.5 scenario (4.68%/5 years). As for the RCP4.5 scenario, B climate is maintained at a similar level in the 2 °C GWL until at the end of the 21st century with narrow ensemble spreads. If we follow the RCP8.5 scenario, meanwhile, the changing pace will be accelerated and increase beyond 40%, compared to the area in the reference period. This implies that if we follow the high-emission scenario, the EA region is projected to experience intense desertification. C and D climates, which are located between increasing types (A, B) and decreasing types (E, F), show a large ensemble spread with no statistically significant linear trends. The areas of C climate exhibit a negative trend under both the RCP4.5 and RCP8.5 scenarios, associated with the "tropicalization" over SA south of 30°N (Figure S4a). Despite a steady increase of C climate area in FEA (Figure S4b), a net decreasing pace of C type is dominant in the CORDEX-EA2 domain (Figure 3c) due to the expansion of A climate over SA (Figure S4a). As for the RCP4.5 scenario, the increasing (0.36%/5 years) and decreasing (−0.38%/5 years) trends are comparable; therefore, the net changing rate is not significant at the 5% significance level. The

key point of this result is that SA will gradually change into tropical climate and C climate over the FEA region will increase under both RCP scenarios. The increase of D climate is mainly due to the large changes from E to D climate (Figure 2a), and this continues increasing under the RCP 4.5 scenario but decreasing under the RCP8.5 scenario. This can be explained with the expansion of C type over FEA, which occurs more prominently under RCP8.5 than under RCP4.5 at the end of the 21st century (Figure S6).

F climate type denotes a rapid decrease to about 45% under the 2 °C GWL, 90% at the 3 °C GWL, and 100% under the RCP8.5 scenario at the end of the 21st century. The changing pace is very fast and substantial under both the RCP 4.5 and RCP8.5 scenarios (Figure 3a), before it reaches the 2 °C GWL. Following the RCP4.5 scenario, the 2 °C GWL will maintain a similar level of change as that with the 1.5 °C GWL, but the continuous decreasing trend of F climate is shown under the RCP8.5 scenario. In addition, the narrower ensemble spread shown in the business-as-usual scenario suggests a high probability of encountering this accelerated decreasing trend and extinction of FT climate.

4. Discussion and Conclusion

The climate changes at target GWLs (2 and 3 °C) are estimated with high-resolution RCM-projected CMIP5 scenarios. The 2 °C GWL is expected to be reached at the mid-21st century (2050s under the RCP4.5 scenario or 2040s under the RCP8.5 scenario), and the 3 °C GWL is expected to be reached at the late 21st century (2070s under only the RCP8.5 scenario). The regional climatic change at each GWL is estimated by the K-T climate classification scheme, which is an effective tool that can be applied easily to climate model data and that considers the change of temperature, precipitation, and their annual cycle within one simple metric.

The FEA region is projected to change from temperate (D) type to subtropical (C) type with increasing HYINT in the coastal regions of the Korean Peninsula, southern Japan, and the middle of the NCP. The 2 °C GWL shows the benefit of preventing the widening of subtropical climate over the Korean Peninsula and southern Japan compared to that of the 3 °C GWL, but not for NCP.

The SA region exhibits the emergence of tropical humid (Aw) climate with a steadily increasing trend until the end of the 21st century whether emission forcing stabilized (RCP4.5) or not (RCP8.5). This changing trend toward warmer and wetter climate could increase the threat to human survivability in relation to heat stress, which is already an issue over SA (Im et al., 2017).

The expansion of arid climate types (Bw and Bs) denotes large scenario dependency over EA. The RCP4.5 scenario retains the 2 °C GWL of change until the end of the 21st century, whereas the RCP8.5 scenario displays the most noticeable increasing rate among K-T climate types. This indicates that the emission scenarios, as well as GWL, are likely to play an important role at regional climate change.

One more remarkable change is shown over the TP region. Almost half of the FT climate area is expected to be changed to various other climate types under the 2 °C GWL and one more degree warming from 2 °C GWL can double the distinction of the FT climate zone, which will reach 100% extinction if we follow the RCP8.5 scenario at the end of the 21st century. The TP is the headwater for the largest rivers in Asia, such as Yellow, Yangtze, and Mekong, and plays a significant role in the hydrological cycle of surrounding countries by reserving water in the forms of snow, glaciers, and permafrost (Ma et al., 2017). Furthermore, the cryosphere (ice and snow) and land that cover this region have a crucial effect on the EA monsoon (Hsu & Liu, 2003; Li et al., 2018; Wang et al., 2008; Wu et al., 2012; Yanai et al., 1992). Therefore, climate changes over the TP region should be studied further.

On the other hand, in interpreting these results, it is necessary to consider the uncertainties that are generally inherent in all future projections. The first one is the small number of ensemble members. High-resolution dynamical downscaling requires intense computational power and human resources. Due to these limitations, the large ensemble of dynamically downscaled regional climate change scenarios needs international cooperation. From this viewpoint, our results offer a preliminary assessment of the CORDEX-EA2 participating ensemble members and should be compared with others in future research. Moreover, our result itself is valuable in suggesting a plausible range of EA climate change attributable to

effective selecting of driving GCMs by considering independency in terms of model genealogy (Knutti et al., 2013) and performance over the EA region (McSweeney et al., 2015).

Another uncertainty comes from the bias correction applied to future projection. To utilize climate model data as input of climate change impact studies, bias correction is unavoidable due to biases in the climate model itself. In the present study, the K-T climate classification scheme also needs realistic climatic values, in terms of not only mean but also their seasonal variations and intensity (minimum/maximum values). However, the validity of bias correction remains controversial in future projections because of its assumption of a "stationary" condition for spatiotemporal variability and its neglect of the relationships between variables (Ehret et al., 2012; Maraun et al., 2017). Therefore, even though QDM, used in this study as the bias correction method, has advantages to overcome temporal stationary assumptions, it should be noted that additional uncertainties can be inherent in any bias-corrected future projection.

The other uncertainty is the limitation in simulating interactions of estimated environmental change with the climate change scenario. For example, following Kang and Eltahir (2018), the NCP region will face the increased risk of heat wave under the RCP8.5 scenario when considering the irrigation-related land-atmosphere interactions. This implies that our result is only a conservative estimation of climate-type changes and the EA region is more likely to suffer severe climate changes if we consider the surface changes and their feedbacks under the same GWL.

The projected spatiotemporal changes of the K-T climate zones at the target GWL over the CORDEX-EA2 domain are expected to be useful not only as vital data for forming a baseline assessment of regional climate change but also an essential tool for disseminating the risk of global warming to the public.

Acknowledgments
This work was funded by the Korea Meteorological Administration Research and Development Program under Grant KMI2018-01213 and "Cooperative Research Program for Agriculture Science & Technology Development (Project No. PJ01229302)" Rural Development Administration, Republic of Korea. We thank Korean Meteorological Administration's supercomputer management division for providing us with the supercomputer resource and for consultation with technical support. The CORDEX-EA phase 2 database can be downloaded from the ESGF node (https://esg-dn1.nsc.liu.se/search/cordex/). The APHRODITE data were obtained from the APHRODITE project data server (http://aphrodite.st.hirosaki-u.ac.jp/download/).

References

Ahn, J. B., Jo, S., Suh, M. S., Cha, D. H., Lee, D. K., Hong, S. Y., et al. (2016). Changes of precipitation extremes over South Korea projected by the 5 RCMs under RCP scenarios. *Asia-Pacific Journal of Atmospheric Sciences*, *52*(2), 223–236. https://doi.org/10.1007/s13143-016-0021-0

Baek, H. J., Lee, J., Lee, H. S., Hyun, Y. K., Cho, C., Kwon, W. T., et al. (2013). Climate change in the 21st century simulated by HadGEM2-AO under representative concentration pathways. *Asia-Pacific Journal of Atmospheric Sciences*, *49*(5), 603–618. https://doi.org/10.1007/s13143-013-0053-7

Belda, M., Holtanová, E., Halenka, T., Kalvová, J., & Hlávka, Z. (2015). Evaluation of CMIP5 present climate simulations using the Köppen-Trewartha climate classification. *Climate Research*, *64*(3), 201–212. https://doi.org/10.3354/cr01316

Bhaskaran, B., Ramachandran, A., Jones, R., & Moufouma-Okia, W. (2012). Regional climate model applications on sub-regional scales over the Indian monsoon region: The role of domain size on downscaling uncertainty. *Journal of Geophysical Research*, *117*, D10113. https://doi.org/10.1029/2012JD017956

Bhatia, K. T., Vecchi, G. A., Knutson, T. R., Murakami, H., Kossin, J., Dixon, K. W., & Whitlock, C. E. (2019). Recent increases in tropical cyclone intensification rates. *Nature Communications*, *10*(1), 1, 635–9. https://doi.org/10.1038/s41467-019-08471-z

Cannon, A. J., Sobie, S. R., & Murdock, T. Q. (2015). Bias correction of GCM precipitation by quantile mapping: How well do methods preserve changes in quantiles and extremes? *Journal of Climate*, *28*(17), 6938–6959. https://doi.org/10.1175/JCLI-D-14-00754.1

Chan, D., & Wu, Q. (2015). Significant anthropogenic-induced changes of climate classes since 1950. *Scientific Reports*, *5*(1), 1–8. https://doi.org/10.1038/srep13487

Chan, D., Wu, Q., Jiang, G., & Dai, X. (2016). Projected shifts in Köppen climate zones over China and their temporal evolution in CMIP5 multi-model simulations. *Advances in Atmospheric Sciences*, *33*(3), 283–293. https://doi.org/10.1007/s00376-015-5077-8

Chen, H., & Sun, J. (2018). Projected changes in climate extremes in China in a 1.5 °C warmer world. *International Journal of Climatology*, *38*(9), 3607–3617. https://doi.org/10.1002/joc.5521

Chen, J., Brissette, F. P., Chaumont, D., & Braun, M. (2013). Finding appropriate bias correction methods in downscaling precipitation for hydrologic impact studies over North America. *Water Resources Research*, *49*, 4187–4205. https://doi.org/10.1002/wrcr.20331

Choi, Y. W., Ahn, J. B., Suh, M. S., Cha, D. H., Lee, D. K., Hong, S. Y., et al. (2016). Future changes in drought characteristics over South Korea using multi regional climate models with the standardized precipitation index. *Asia-Pacific Journal of Atmospheric Sciences*, *52*(2), 209–222. https://doi.org/10.1007/s13143-016-0020-1

Collins, M., Knutti, R., Arblaster, J., Dufresne, J.-L., Fichefet, T., Friedlingstein, P., et al. (2013). Long-term climate change: Projections, commitments and irreversibility pages 1029 to 1076. In *Intergovernmental Panel on Climate Change (Ed.), Climate Change 2013—The Physical Science Basis* (Vol. 9781107057, pp. 1029–1136). Cambridge: Cambridge University Press. https://doi.org/10.1017/CBO9781107415324.024

De Castro, M., Gallardo, C., Jylha, K., & Tuomenvirta, H. (2007). The use of a climate-type classification for assessing climate change effects in Europe from an ensemble of nine regional climate models. *Climatic Change*, *81*(SUPPL. 1), 329–341. https://doi.org/10.1007/s10584-006-9224-1

Donnelly, C., Greuell, W., Andersson, J., Gerten, D., Pisacane, G., Roudier, P., & Ludwig, F. (2017). Impacts of climate change on European hydrology at 1.5, 2 and 3 degrees mean global warming above preindustrial level. *Climatic Change*, *143*(1–2), 13–26. https://doi.org/10.1007/s10584-017-1971-7

Dosio, A., & Fischer, E. M. (2018). Will half a degree make a difference? Robust projections of indices of mean and extreme climate in Europe under 1.5°C, 2°C, and 3°C global warming. *Geophysical Research Letters*, *45*, 935–944. https://doi.org/10.1002/2017GL076222

Ehret, U., Zehe, E., Wulfmeyer, V., Warrach-Sagi, K., & Liebert, J. (2012). HESS opinions "should we apply bias correction to global and regional climate model data?". *Hydrology and Earth System Sciences*, *16*(9), 3391–3404. https://doi.org/10.5194/hess-16-3391-2012

Eum, H. I., & Cannon, A. J. (2017). Intercomparison of projected changes in climate extremes for South Korea: Application of trend preserving statistical downscaling methods to the CMIP5 ensemble. *International Journal of Climatology*, *37*(8), 3381–3397. https://doi.org/10.1002/joc.4924

Evans, J. P., & McCabe, M. F. (2013). Effect of model resolution on a regional climate model simulation over southeast Australia. *Climate Research*, *56*, 131–145. https://doi.org/10.3354/cr01151

Feng, S., Ho, C. H., Hu, Q., Oglesby, R. J., Jeong, S. J., & Kim, B. M. (2012). Evaluating observed and projected future climate changes for the Arctic using the Köppen-Trewartha climate classification. *Climate Dynamics*, *38*(7–8), 1359–1373. https://doi.org/10.1007/s00382-011-1020-6

Gallardo, C., Gil, V., Hagel, E., Tejeda, C., & de Castro, M. (2013). Assessment of climate change in Europe from an ensemble of regional climate models by the use of Köppen-Trewartha classification. *International Journal of Climatology*, *33*(9), 2157–2166. https://doi.org/10.1002/joc.3580

Gao, X., & Giorgi, F. (2008). Increased aridity in the Mediterranean region under greenhouse gas forcing estimated from high resolution simulations with a regional climate model. *Global and Planetary Change*, *62*(3–4), 195–209. https://doi.org/10.1016/j.gloplacha.2008.02.002

Ge, F., Zhu, S., Peng, T., Zhao, Y., Sielmann, F., Fraedrich, K., et al. (2019). Risks of precipitation extremes over Southeast Asia: Does 1.5 °C or 2 °C global warming make a difference? *Environmental Research Letters*, *14*(4), 044015. https://doi.org/10.1088/1748-9326/aaff7e

Giorgetta, M. A., Jungclaus, J., Reick, C. H., Legutke, S., Bader, J., Böttinger, M., et al. (2013). Climate and carbon cycle changes from 1850 to 2100 in MPI-ESM simulations for the Coupled Model Intercomparison Project phase 5. *Journal of Advances in Modeling Earth Systems*, *5*, 572–597. https://doi.org/10.1002/jame.20038

Giorgi, F., Coppola, E., Raffaele, F., Diro, G. T., Fuentes-Franco, R., Giuliani, G., et al. (2014). Changes in extremes and hydroclimatic regimes in the CREMA ensemble projections. *Climatic Change*, *125*(1), 39–51. https://doi.org/10.1007/s10584-014-1117-0

Giorgi, F., Im, E. S., Coppola, E., Diffenbaugh, N. S., Gao, X. J., Mariotti, L., & Shi, Y. (2011). Higher hydroclimatic intensity with global warming. *Journal of Climate*, *24*(20), 5309–5324. https://doi.org/10.1175/2011JCLI3979.1

Hagemann, S., Chen, C., Haerter, J. O., Heinke, J., Gerten, D., & Piani, C. (2011). Impact of a statistical bias correction on the projected hydrological changes obtained from three GCMs and two hydrology models. *Journal of Hydrometeorology*, *12*(4), 556–578. https://doi.org/10.1175/2011JHM1336.1

Hawkins, E., Ortega, P., Suckling, E., Schurer, A., Hegerl, G., Jones, P., et al. (2017). Estimating changes in global temperature since the preindustrial period. *Bulletin of the American Meteorological Society*, *98*(9), 1841–1856. https://doi.org/10.1175/BAMS-D-16-0007.1

Hsu, H. H., & Liu, X. (2003). Relationship between the Tibetan Plateau heating and East Asian summer monsoon rainfall. *Geophysical Research Letters*, *30*(20), 2066. https://doi.org/10.1029/2003GL017909

Im, E. S., Ahn, J. B., & Jo, S. R. (2015). Regional climate projection over South Korea simulated by the HadGEM2-AO and WRF model chain under RCP emission scenarios. *Climate Research*, *63*(3), 249–266. https://doi.org/10.3354/cr01292

Im, E. S., Choi, Y. W., & Ahn, J. B. (2017). Robust intensification of hydroclimatic intensity over East Asia from multi-model ensemble regional projections. *Theoretical and Applied Climatology*, *129*(3–4), 1241–1254. https://doi.org/10.1007/s00704-016-1846-2

Im, E. S., Kwon, W. T., Ahn, J. B., & Giorgi, F. (2007). Multi-decadal scenario simulation over Korea using a one-way double-nested regional climate model system. Part 1: Recent climate simulation(1971-2000). *Climate Dynamics*, *28*(7–8), 759–780. https://doi.org/10.1007/s00382-006-0203-z

Im, E.-S., Nguyen-xuan, T., Kim, Y.-H., & Ahn, J.-B. (2019). 2018 summer extreme temperatures in South Korea and their intensification under 3°C global warming. *Environmental Research Letters*, *31*(5), 845–851. https://doi.org/10.1088/1748-9326/ab3b8f

Im, E. S., Pal, J. S., & Eltahir, E. A. B. (2017). Deadly heat waves projected in the densely populated agricultural regions of South Asia. *Science Advances*, *3*(8), 1, e1603322–8. https://doi.org/10.1126/sciadv.1603322

Im, E. S., Park, E. H., Kwon, W. T., & Giorgi, F. (2006). Present climate simulation over Korea with a regional climate model using a one-way double-nested system. *Theoretical and Applied Climatology*, *86*(1–4), 187–200. https://doi.org/10.1007/s00704-005-0215-3

Intergovernmental Panel on Climate Change (2018). Global warming of 1.5° C: An IPCC special report on the impacts of global warming of 1.5° C above pre-industrial levels and related global greenhouse gas emission pathways, in the context of strengthening the global response to the threat of climate change, sustainable development, and efforts to eradicate poverty. Intergovernmental Panel on Climate Change.

Jacob, D., Kotova, L., Teichmann, C., Sobolowski, S. P., Vautard, R., Donnelly, C., et al. (2018). Climate impacts in Europe under +1.5°C global warming. *Earth's Future*, *6*(2), 264–285. https://doi.org/10.1002/2017EF000710

James, R., Washington, R., Schleussner, C. F., Rogelj, J., & Conway, D. (2017). Characterizing half-a-degree difference: A review of methods for identifying regional climate responses to global warming targets. *Wiley Interdisciplinary Reviews: Climate Change*, *8*(2). https://doi.org/10.1002/wcc.457

Joshi, M., Hawkins, E., Sutton, R., Lowe, J., & Frame, D. (2011). Projections of when temperature change will exceed 2°C above pre-industrial levels. *Nature Climate Change*, *1*(8), 407–412. https://doi.org/10.1038/nclimate1261

Kang, S., & Eltahir, E. A. B. (2018). North China Plain threatened by deadly heatwaves due to climate change and irrigation. *Nature Communications*, *9*(1), 2894. https://doi.org/10.1038/s41467-018-05252-y

Karl, T. R., Nicholls, N., & Ghazi, A. (1999). CLIVAR/GCOS/WMO workshop on indices and indicators for climate extremes workshop summary BT—Weather and climate extremes: Changes, variations and a perspective from the insurance industry. In *Weather and climate extremes* (pp. 3–7). Dordrecht: Springer Netherlands. https://doi.org/10.1007/978-94-015-9265-9_2

Karmalkar, A. V., & Bradley, R. S. (2017). Consequences of global warming of 1.5 °C and 2 °C for regional temperature and precipitation changes in the contiguous United States. *PLoS ONE*, *12*(1), 1, e0168697–17. https://doi.org/10.1371/journal.pone.0168697

King, A. D., & Karoly, D. J. (2017). Climate extremes in Europe at 1.5 and 2 degrees of global warming. *Environmental Research Letters*, *12*(11). https://doi.org/10.1088/1748-9326/aa8e2c

King, A. D., Karoly, D. J., & Henley, B. J. (2017). Australian climate extremes at 1.5 °C and 2 °C of global warming. *Nature Climate Change*, *7*(6), 412–416. https://doi.org/10.1038/nclimate3296

Kirtman, B., Power, S. B., Adedoyin, J. A., Boer, G. J., Bojariu, R., Camilloni, I., et al. (2013). Near-term climate change: Projections and predictability. In *Intergovernmental Panel on Climate Change (Ed.), Climate change 2013: The physical science basis: Working Group I Contribution to the Fifth Assessment Report of the Intergovernmental Panel on Climate Change* (Vol. 9781107057, pp. 953–1028). Cambridge: Cambridge University Press. https://doi.org/10.1017/CBO9781107415324.023

Knutti, R., Masson, D., & Gettelman, A. (2013). Climate model genealogy: Generation CMIP5 and how we got there. *Geophysical Research Letters*, *40*, 1194–1199. https://doi.org/10.1002/grl.50256

Knutti, R., & Rogelj, J. (2015). The legacy of our CO_2 emissions: A clash of scientific facts, politics and ethics. *Climatic Change*, *133*(3), 361–373. https://doi.org/10.1007/s10584-015-1340-3

Köppen, W. (1936). Das geographische System der Klimate. In W. Köppen & R. Geiger (Eds.), *Handbuch der Klimato - logie* (pp. 1–44). Berlin: Gebrüder Borntraeger.
Leduc, M., & Laprise, R. (2009). Regional climate model sensitivity to domain size. *Climate Dynamics*, *32*, 833–854. https://doi.org/10.1007/s00382-008-0400-z
Lee, D., Min, S. K., Fischer, E., Shiogama, H., Bethke, I., Lierhammer, L., & Scinocca, J. F. (2018). Impacts of half a degree additional warming on the Asian summer monsoon rainfall characteristics. *Environmental Research Letters*, *13*(4), 044033. https://doi.org/10.1088/1748-9326/aab55d
Lee, H., Kim, G., Park, C., & Cha, D.-H. (2017). A study of future changes of climate classification and extreme temperature events over South Korea in multi regional climate model simulations. *Climate Research*, *12*, 149–164. (in Korean with English abstract)
Lee, J. W., & Hong, S. Y. (2014). Potential for added value to downscaled climate extremes over Korea by increased resolution of a regional climate model. *Theoretical and Applied Climatology*, *117*(3–4), 667–677. https://doi.org/10.1007/s00704-013-1034-6
Lee, S. M., & Min, S. K. (2018). Heat stress changes over East Asia under 1.5° and 2.0°C global warming targets. *Journal of Climate*, *31*(7), 2819–2831. https://doi.org/10.1175/JCLI-D-17-0449.1
Lennard, C. J., Nikulin, G., Dosio, A., & Moufouma-Okia, W. (2018). On the need for regional climate information over Africa under varying levels of global warming. *Environmental Research Letters*, *13*(6), 060401. https://doi.org/10.1088/1748-9326/aab2b4
Lewis, S. C., King, A. D., & Mitchell, D. M. (2017). Australia's unprecedented future temperature extremes under Paris limits to warming. *Geophysical Research Letters*, *44*, 9947–9956. https://doi.org/10.1002/2017GL074612
Li, W., Guo, W., Qiu, B., Xue, Y., Hsu, P. C., & Wei, J. (2018). Influence of Tibetan Plateau snow cover on East Asian atmospheric circulation at medium-range time scales. *Nature Communications*, *9*(1), 4243. https://doi.org/10.1038/s41467-018-06762-5
Ma, Y., Ma, W., Zhong, L., Hu, Z., Li, M., Zhu, Z., et al. (2017). Monitoring and modeling the Tibetan Plateau's climate system and its impact on East Asia. *Scientific Reports*, *7*(1), 44574. https://doi.org/10.1038/srep44574
Mahlstein, I., Daniel, J. S., & Solomon, S. (2013). Pace of shifts in climate regions increases with global temperature. *Nature Climate Change*, *3*(8), 739–743. https://doi.org/10.1038/nclimate1876
Maraun, D., Shepherd, T. G., Widmann, M., Zappa, G., Walton, D., Gutiérrez, J. M., et al. (2017). Towards process-informed bias correction of climate change simulations. *Nature Climate Change*, *7*(11), 764–773. https://doi.org/10.1038/nclimate3418
Marx, A., Kumar, R., Thober, S., Rakovec, O., Wanders, N., Zink, M., et al. (2018). Climate change alters low flows in Europe under global warming of 1.5, 2, and 3°C. *Hydrology and Earth System Sciences*, *22*(2), 1017–1032. https://doi.org/10.5194/hess-22-1017-2018
Masson, D., & Knutti, R. (2011). Climate model genealogy. *Geophysical Research Letters*, *38*, L08703. https://doi.org/10.1029/2011GL046864
Maúre, G., Pinto, I., Ndebele-Murisa, M., Muthige, M., Lennard, C., Nikulin, G., et al. (2018). The southern African climate under 1.5 °C and 2 °C of global warming as simulated by CORDEX regional climate models. *Environmental Research Letters*, *13*(6), 065002. https://doi.org/10.1088/1748-9326/aab190
Maurer, E. P., & Pierce, D. W. (2014). Bias correction can modify climate model simulated precipitation changes without adverse effect on the ensemble mean. *Hydrology and Earth System Sciences*, *18*(3), 915–925. https://doi.org/10.5194/hess-18-915-2014
Mauritsen, T., & Pincus, R. (2017). Committed warming inferred from observations. *Nature Climate Change*, *7*(9), 652–655. https://doi.org/10.1038/nclimate3357
Mba, W. P., Longandjo, G. N. T., Moufouma-Okia, W., Bell, J. P., James, R., Vondou, D. A., et al. (2018). Consequences of 1.5 °C and 2 °C global warming levels for temperature and precipitation changes over Central Africa. *Environmental Research Letters*, *13*(5). https://doi.org/10.1088/1748-9326/aab048
McSweeney, C. F., Jones, R. G., Lee, R. W., & Rowell, D. P. (2015). Selecting CMIP5 GCMs for downscaling over multiple regions. *Climate Dynamics*, *44*(11–12), 3237–3260. https://doi.org/10.1007/s00382-014-2418-8
Nikulin, G., Lennard, C., Dosio, A., Kjellström, E., Chen, Y., Hansler, A., et al. (2018). The effects of 1.5 and 2 degrees of global warming on Africa in the CORDEX ensemble. *Environmental Research Letters*, *13*(6). https://doi.org/10.1088/1748-9326/aab1b1
Nkemelang, T., New, M., & Zaroug, M. (2018). Temperature and precipitation extremes under current, 1.5 °C and 2.0 °C global warming above pre-industrial levels over Botswana, and implications for climate change vulnerability. *Environmental Research Letters*, *13*(6). https://doi.org/10.1088/1748-9326/aac2f8
Osima, S., Indasi, V. S., Zaroug, M., Endris, H. S., Gudoshava, M., Misiani, H. O., et al. (2018). Projected climate over the Greater Horn of Africa under 1.5 °C and 2 °C global warming. *Environmental Research Letters*, *13*(6), 065004. https://doi.org/10.1088/1748-9326/aaba1b
Peterson, T. C., Folland, C. C., Gruza, G., Hogg, W., Mokssit, A., & Plummer, N.(2001). Report on the activities of the Working Group on Climate Change Detection and Related Rapporteurs 1998–2001. Rep. WCDMP-47, WMO-TD 1071,(March), 143. https://doi.org/WMO, Rep. WCDMP-47,WMO-TD 1071
Prajapat, D. K., Lodha, J., & Choudhary, M. (2019). A spatiotemporal analysis of Indian warming target using CORDEX-SA experiment data. *Theoretical and Applied Climatology*, 1–13. https://doi.org/10.1007/s00704-019-02978-7
Raftery, A. E., Zimmer, A., Frierson, D. M. W., Startz, R., & Liu, P. (2017). Less than 2 °C warming by 2100 unlikely. *Nature Climate Change*, *7*(9), 637–641. https://doi.org/10.1038/nclimate3352
Rajaud, A., & de Noblet-Ducoudré, N. (2017). Tropical semi-arid regions expanding over temperate latitudes under climate change. *Climatic Change*, *144*(4), 703–719. https://doi.org/10.1007/s10584-017-2052-7
Rogelj, J., den Elzen, M., Höhne, N., Fransen, T., Fekete, H., Winkler, H., et al. (2016). Paris Agreement climate proposals need a boost to keep warming well below 2 °C. *Nature*, *534*(7609), 631–639. https://doi.org/10.1038/nature18307
Sandel, B., Arge, L., Dalsgaard, B., Davies, R. G., Gaston, K. J., Sutherland, W. J., & Svenning, J. C. (2011). The influence of late quaternary climate-change velocity on species endemism. *Science*, *334*(6056), 660–664. https://doi.org/10.1126/science.1210173
Seneviratne, S. I., Donat, M. G., Pitman, A. J., Knutti, R., & Wilby, R. L. (2016). Allowable CO_2 emissions based on regional and impact-related climate targets. *Nature*, *529*(7587), 477–483. https://doi.org/10.1038/nature16542
Sherwood, S. C., & Huber, M. (2010). An adaptability limit to climate change due to heat stress. *Proceedings of the National Academy of Sciences of the United States of America*, *107*(21), 9552–9555. https://doi.org/10.1073/pnas.0913352107
Shi, Y., Gao, X.-J., & Wu, J. (2012). Projected changes in Köppen climate types in the 21st century over China. *Atmospheric and Oceanic Science Letters*, *5*(6), 495–498. https://doi.org/10.1080/16742834.2012.11447043
Shi, Y., Zhang, D. F., Xu, Y., & Zhou, B. T. (2018). Changes of heating and cooling degree days over China in response to global warming of 1.5 °C, 2 °C, 3 °C and 4 °C. *Advances in Climate Change Research*, *9*(3), 192–200. https://doi.org/10.1016/j.accre.2018.06.003
Sillmann, J., Kharin, V. V., Zwiers, F. W., Zhang, X., & Bronaugh, D. (2013). Climate extremes indices in the CMIP5 multimodel ensemble: Part 2. Future climate projections. *Journal of Geophysical Research – Atmospheres*, *118*, 2473–2493. https://doi.org/10.1002/jgrd.50188

Sun, H., Wang, A., Zhai, J., Huang, J., Wang, Y., Wen, S., et al. (2018). Impacts of global warming of 1.5 °C and 2.0 °C on precipitation patterns in China by regional climate model (COSMO-CLM). *Atmospheric Research*, *203*, 83–94. https://doi.org/10.1016/j.atmosres.2017.10.024

Swain, S., & Hayhoe, K. (2015). CMIP5 projected changes in spring and summer drought and wet conditions over North America. *Climate Dynamics*, *44*(9–10), 2737–2750. https://doi.org/10.1007/s00382-014-2255-9

Sylla, M. B., Faye, A., Giorgi, F., Diedhiou, A., & Kunstmann, H. (2018). Projected heat stress under 1.5 °C and 2 °C global warming scenarios creates unprecedented discomfort for humans in West Africa. *Earth's Future*, *6*(7), 1029–1044. https://doi.org/10.1029/2018EF000873

Sylla, M. B., Pal, J. S., Faye, A., Dimobe, K., & Kunstmann, H. (2018). Climate change to severely impact West African basin scale irrigation in 2 °C and 1.5 °C global warming scenarios. *Scientific Reports*, *8*(1), 1–9. https://doi.org/10.1038/s41598-018-32736-0

Talchabhadel, R., & Karki, R. (2019). Assessing climate boundary shifting under climate change scenarios across Nepal. *Environmental Monitoring and Assessment*, *191*(8), 520.

Teutschbein, C., & Seibert, J. (2012). Bias correction of regional climate model simulations for hydrological climate-change impact studies: Review and evaluation of different methods. *Journal of Hydrology*, *456–457*, 12–29. https://doi.org/10.1016/j.jhydrol.2012.05.052

Trewartha, G. T., & Horn, L. H. (1980). *An introduction to climate*, (5th ed.). New York, NY: McGraw-Hill Book Co.

United Nations(2015) Paris agreement.(https://unfccc.int/sites/default/files/english_paris_agreement.pdf)

van Vuuren, D. P., Edmonds, J., Kainuma, M., Riahi, K., Thomson, A., Hibbard, K., et al. (2011). The representative concentration pathways: An overview. *Climatic Change*, *109*(1-2), 5–31. https://doi.org/10.1007/s10584-011-0148-z

Vautard, R., Gobiet, A., Sobolowski, S., Kjellström, E., Stegehuis, A., Watkiss, P., et al. (2014). The European climate under a 2 °C global warming. *Environmental Research Letters*, *9*(3), 034006. https://doi.org/10.1088/1748-9326/9/3/034006

Wang, B., Bao, Q., Hoskins, B., Wu, G., & Liu, Y. (2008). Tibetan Plateau warming and precipitation changes in East Asia. *Geophysical Research Letters*, *35*, L14702. https://doi.org/10.1029/2008GL034330

Wang, B., & Lin, H. (2002). Rainy season of the Asian–Pacific summer monsoon. *Journal of Climate*, *15*, 386–398.

Wu, Z., Li, J., Jiang, Z., & Ma, T. (2012). Modulation of the Tibetan Plateau snow cover on the ENSO teleconnections: From the East Asian summer monsoon perspective. *Journal of Climate*, *25*(7), 2481–2489. https://doi.org/10.1175/JCLI-D-11-00135.1

Xu, Y., Zhou, B. T., Wu, J., Han, Z. Y., Zhang, Y. X., & Wu, J. (2017). Asian climate change under 1.5–4 °C warming targets. *Advances in Climate Change Research*, *8*(2), 99–107. https://doi.org/10.1016/j.accre.2017.05.004

Yanai, M., Li, C., & Song, Z. (1992). Seasonal heating of the Tibetan Plateau and its effects on the evolution of the Asian summer monsoon. *Journal of the Meteorological Society of Japan*, *70*(1), 319–351. https://doi.org/10.2151/jmsj1965.70.1B_319

Yatagai, A., Kamiguchi, K., Arakawa, O., Hamada, A., Yasutomi, N., & Kitoh, A. (2012). APHRODITE: Constructing a long-term daily gridded precipitation dataset for Asia based on a dense network of rain gauges. *Bulletin of the American Meteorological Society*, *93*(9), 1401–1415. https://doi.org/10.1175/BAMS-D-11-00122.1

Yun, K. S., Heo, K. Y., Chu, J. E., Ha, K. J., Lee, E. J., Choi, Y., & Kitoh, A. (2012). Changes in climate classification and extreme climate indices from a high-resolution future projection in Korea. Asia-Pacific J. *Atmospheric Sciences*, *48*(3), 213–226. https://doi.org/10.1007/s13143-012-0022-6

Žagar, N., Honzak, L., Žabkar, R., Skok, G., Rakovec, J., & Ceglar, A. (2013). Uncertainties in a regional climate model in the midlatitudes due to the nesting technique and the domain size. *Journal of Geophysical Research – Atmospheres*, *118*, 6189–6199. https://doi.org/10.1002/jgrd.50525

Zeroual, A., Assani, A. A., Meddi, M., & Alkama, R. (2019). Assessment of climate change in Algeria from 1951 to 2098 using the Köppen–Geiger climate classification scheme. *Climate Dynamics*, *52*(1–2), 227–243. https://doi.org/10.1007/s00382-018-4128-0

Zhao, S., & Zhou, T. (2019). Are the observed changes in heat extremes associated with a half-degree warming increment analogues for future projections? *Earth's Future.*, *7*(8), 978–992. https://doi.org/10.1029/2019EF001237

References From the Supporting Information

Patton, C. P. (1962). A note on the classification of dry climate in the Köppen system. *Geography of California*, *3*, 105–112.